

# Non-resonant Raman Spectroscopy of Individual ZnO Nanowires *via* Au Nanorod Surface Plasmons

*Andrea Pescaglino,<sup>a</sup> Eleonora Secco,<sup>b</sup> Alfonso Martin,<sup>a</sup> Davide Cammi,<sup>c</sup> Carsten Ronning,<sup>c</sup>  
Andrés Cantarero,<sup>b</sup> Nuria Garro<sup>b</sup> and Daniela Iacopino<sup>a</sup>*

<sup>a</sup> Tyndall National Institute – University College Cork, Lee Maltings, Cork, Ireland

<sup>b</sup> Institute of Materials Science, University of Valencia, Valencia, Spain

<sup>c</sup> Institute of Solid State Physics, Friedrich Schiller University of Jena, Max-Wien-Platz 1, 07743  
Jena, Germany

## **Optical properties of Au nanorods**

Colloidal Au nanorods, which were synthesized by a seed-mediated method, show a transversal plasmon resonance (TPR) centered at 524 nm and a longitudinal plasmon resonance (LPR) centered at 657 nm (Figure S1). A representative SEM image of the synthesized Au nanorods having mean diameter and length of  $29 \pm 5$  nm and  $68 \pm 5$  nm, respectively (averaged over 100 nanorods) is shown in the inset of Figure S1.

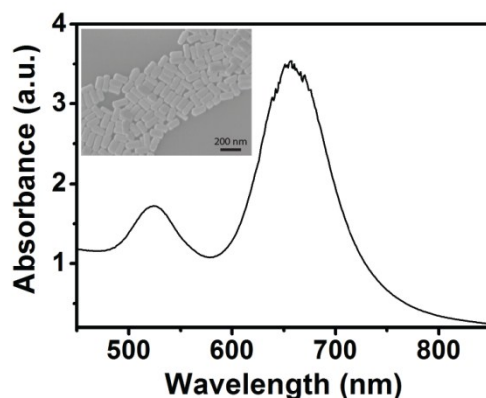
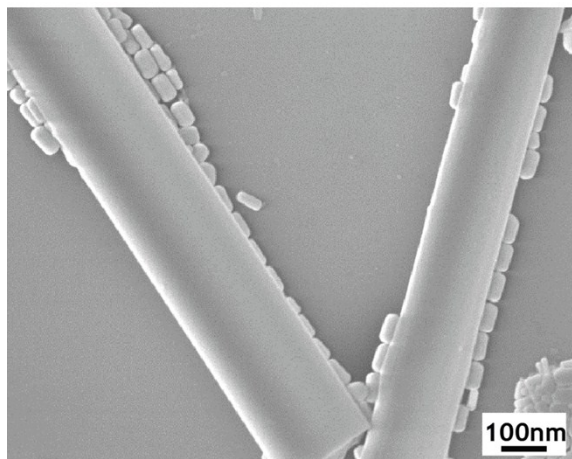


**Figure S1.** Absorbance spectrum of Au nanorods dispersed in water solution. Inset: SEM image of the synthesized Au nanorods deposited on Si/SiO<sub>2</sub> substrate.

### **Mask selective droplet deposition**

Hybrid nanostructures were fabricated by mask-selective droplet deposition. Two approaches were used to etch the photoresist deposited on ZnO nanowires in a controlled manner. The obtained samples were used for statistical analysis and were called hybrids A and B. The first approach is described in detail in the manuscript text and relies on the controlled etching of photoresist by O<sub>2</sub>-plasma (hybrids A). This technique provided a reliable and reproducible method to control the photoresist thickness with accuracy of ~30 nm. The second approach is based on a lithography process, where the photoresist was firstly exposed to UV light and subsequently partially removed by a photoresist developer.<sup>1</sup> The desired thickness of the residual layer was achieved by optimizing the exposition and development time and was found reproducible within ~50 nm for thicknesses above ~100 nm. Compared to the former this process allows a more efficient removal of the photoresist from the nanowire without potential damaging of the surface.

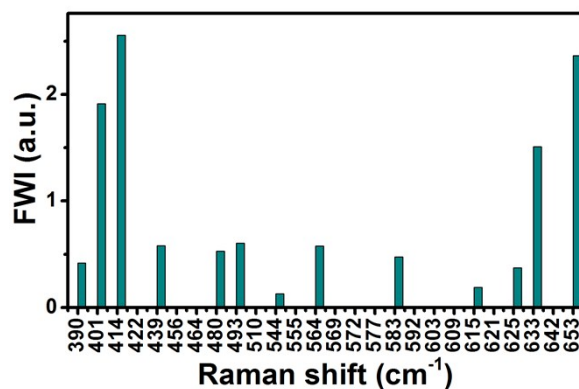
SEM image of Figure S2 shows that nanorods deposited on ZnO without photoresist layer accumulated on the substrate adjacent to the nanowire, leaving the nanowire surface uncovered.



**Figure S2.** SEM image of Au nanorods deposited by direct droplet deposition on a SiO<sub>2</sub> substrate containing ZnO nanowires.

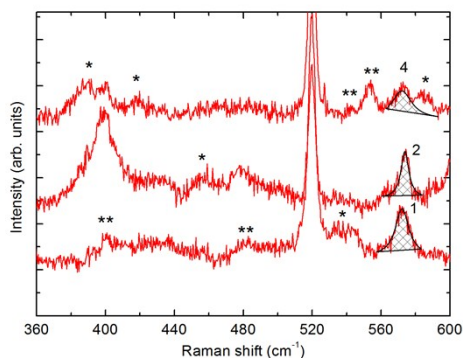
### Statistical analysis of Raman spectra

Figure S3 reports on statistical analysis of Raman peaks found in 20 spectra of Au nanorods deposited on Si/SiO<sub>2</sub>. Obtained peaks were attributed to excess CTAB molecules used in the Au nanorod synthesis.



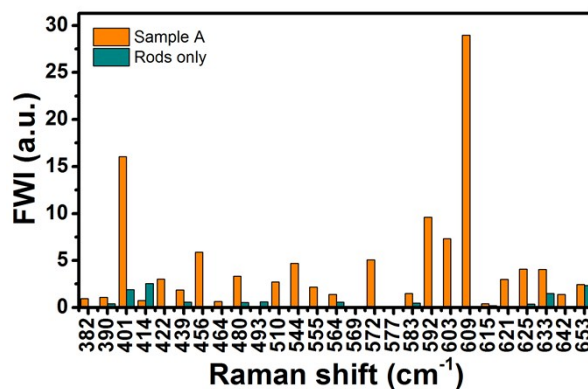
**Figure S3.** Statistical analysis of Raman peaks found in 20 spectra of Au nanorods deposited via droplet deposition on Si/SiO<sub>2</sub>.

Figure S4 shows three representative Raman spectra obtained from Au nanorods – ZnO nanowire structures obtained by O<sub>2</sub>-plasma mask-selective droplet deposition. Under illumination at 647 nm all samples showed a reproducible peak at 572 cm<sup>-1</sup> attributed to the ZnO SO mode. The asterisks indicate the peaks attributed to crystalline CTAB. The double asterisks mark peaks were also found in blank samples constituted by Au nanorods deposited on Si/SiO<sub>2</sub> substrate, and therefore were not attributable to ZnO.



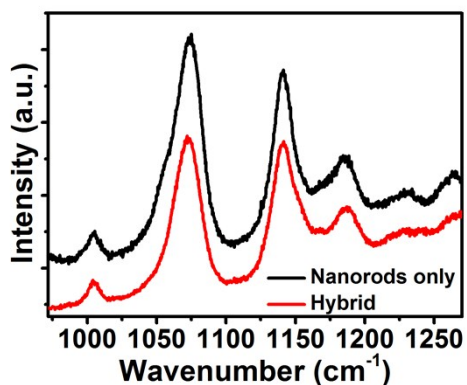
**Figure S4.** Raman spectra of hybrid Au nanorods – ZnO nanowire nanostructures illuminated at 647 nm. The black lines are the fit of SO mode peaks centred at 572 cm<sup>-1</sup>.

Figure S5 shows statistical data of all Raman signals collected for 10 Au nanorods – ZnO nanowire hybrid structures (hybrids A, orange histograms). For comparison the statistical data collected from 20 samples of Au nanorods deposited on Si/SiO<sub>2</sub> substrates were also added.



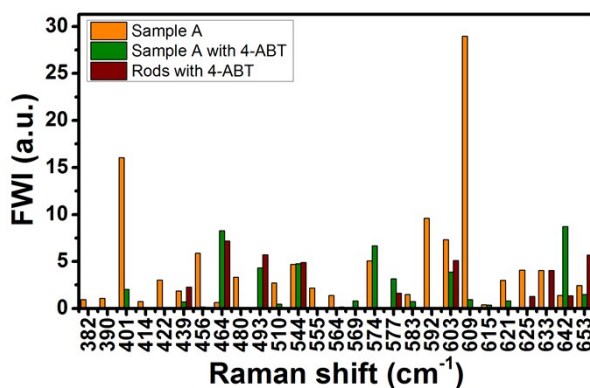
**Figure S5.** Statistical analysis obtained from Sample A and Au nanorods deposited on Si/SiO<sub>2</sub>.

Figure S6 shows representative Raman spectra recorded on a hybrid nanostructure (red line) and on Au nanorods deposited on Si/SiO<sub>2</sub> substrate (black line) after immersion in 4-ABT. The peaks at 1004, 1073, 1139 and 1187 cm<sup>-1</sup> show distinctive 4-ABT Raman transitions<sup>2,3</sup> demonstrate the successful attachment of the 4-ABT molecule on the nanorods surface.



**Figure S6.** Representative Raman spectra recorded on a hybrid device (red line) and on Au nanorods deposited on Si/SiO<sub>2</sub> substrate (black line) after immersion in 4-ABT.

Figure S7 shows statistical analysis of peaks found in Au nanorods – ZnO nanowire hybrid structures (hybrids A, orange histograms). The statistic also report peaks obtained from the same hybrids A after immersion in 4-ABT (green histograms). For comparison, peaks obtained from Au nanorods after immersion in 4-ABT are also reported (brown histogram). 4-ABT was used to substitute CTAB molecules bound on the surface of Au nanorods. 10 spectra per each sample were used to build the statistical data.



**Figure S7.** Statistical analysis obtained from hybrids A, hybrids A after immersion in 4-ABT and Au nanorods deposited on Si/SiO<sub>2</sub> substrate after immersion in 4-ABT.

## References

- 1 A. Pescaglini, A. Martín, D. Cammi, G. Juska, C. Ronning, E. Pelucchi and D. Iacopino, *Nano Lett.*, 2014, DOI: 10.1021/nl5024854.
- 2 A. Martín, A. Pescaglini, C. Schopf, V. Scardaci, R. Coull, L. Byrne and D. Iacopino, *J. Phys. Chem. C*, 2014, **118**, 13260-13267.
- 3 M. Osawa, N. Matsuda, K. Yoshii and I. Uchida, *The Journal of Physical Chemistry*, 1994, **98**, 12702-12707.